PHYSICAL REVIEW B **70**, 165103 (2004)

Single Mott transition in the multiorbital Hubbard model

A. Liebsch*
Institut für Festkörperforschung, Forschungszentrum Jülich, 52425 Jülich, Germany
(Received 18 May 2004; published 12 October 2004; corrected 10 November 2004)

The Mott transition in a multiorbital Hubbard model involving subbands of different widths is studied within the dynamical mean-field theory. Using the iterated perturbation theory for the quantum impurity problem it is shown that at low temperatures interorbital Coulomb interactions give rise to a single first-order transition rather than a sequence of orbital selective transitions. Impurity calculations based on the Quantum Monte Carlo method confirm this qualitative behavior. Nevertheless, at finite temperatures, the degree of metallic or insulating behavior of the subbands differs greatly. Thus, on the metallic side of the transition, the narrow band can exhibit quasi-insulating features, whereas on the insulating side the wide band exhibits pronounced bad-metal behavior. This complexity might partly explain contradictory results between several previous works.

DOI: 10.1103/PhysRevB.70.165103 PACS number(s): 71.20.Be, 71.27.+a, 79.60.Bm

I. INTRODUCTION

The nature of the metal insulator transition in multiband materials involving subbands of different widths is not yet fully understood. As a result of the geometric complexity of many transition metal oxides, the degeneracy of valence bands is frequently lifted, giving rise to coexisting narrow and wide partially filled bands. A key issue in these materials is therefore whether these subbands exhibit separate Mott transitions or whether single-particle hybridization among subbands and interorbital Coulomb interactions ensure the occurrence of a single transition involving all subbands simultaneously. An example is the layer perovskite Sr_2RuO_4 which consists of a wide, two-dimensional d_{xy} band and narrow, nearly one-dimensional $d_{xz,yz}$ bands.[1] This system is believed to exhibit unconventional p-wave superconductivity.[2] Isoelectronic replacement of Sr by Ca leads to a distortion of oxygen octahedra and an effective narrowing of the Ru-derived t_{2g} bands, causing a metal insulator transition.[3] Another case is the layer compound Na_xCoO_2 which as a function of doping concentration exhibits a wide range of properties, including superconductivity (when hydrated), while the parent material CoO_2 is an insulator.[4]

In previous work[5] we investigated the Mott transition in $Ca_{2-x}Sr_xRuO_4$ by considering a three-band model appropriate for Sr_2RuO_4 and varying the on-site Coulomb interaction rather than modifying the band width. Extending earlier quasiparticle calculations for this system[6] within the dynamical mean-field theory[7] (DMFT) we found that interorbital Coulomb interactions lead to a significant redistribution of spectral weight between t_{2g} orbitals. As a result, despite the completely different shapes and widths of the single-particle densities of states, for increasing U the d_{xy} and $d_{xz,yz}$ subbands exhibit similar correlation features, suggesting the existence of a single Mott transition. Additional single-particle coupling between t_{2g} states caused by octahedral distortions[8] undoubtedly will enhance the trend towards a single transition. This result was in conflict with DMFT calculations by Anisimov *et al.*[9] who obtained a sequence of Mott transitions as the on-site Coulomb interaction was increased beyond the single-particle widths of the narrow and wide t_{2g} subbands of Sr_2RuO_4, respectively.

To avoid the uncertainties stemming from the maximum entropy reconstruction[10] of real-frequency spectra we recently considered a simple two-band model and focused on quantities directly available from the Quantum Monte Carlo (QMC) calculations carried out at imaginary times and frequencies.[11] The subbands were assumed to have semicircular density of states of widths $W_1=2$ eV, $W_2=4$ eV, to be each half filled, and to interact only via local intraorbital and interorbital Coulomb energies U and $U'=U-2J$, where J is the Hund's rule exchange integral. The quantum impurity calculations were performed within the DMFT and multiorbital QMC method for $T=125$ meV. For increasing U and U' (with fixed $J=0.2$ eV) the subband quasiparticle weights Z_i were found to vanish at about the same critical U_c, within a characteristic uncertainty caused by critical slowing down. The same behavior was found for the quantities $G_i(\beta/2)$ $(\beta=1/k_BT)$ which define the spectral weight of the coherent subband peaks within a few k_BT of E_F. Also, two-band calculations at $T=0$ within the iterated perturbation theory[12] (IPT) supported the existence of a common transition. These results confirmed our previous finding, namely, that intersubband coupling due to local Coulomb interactions gives rise to a single Mott transition rather than a sequence of orbital-selective transitions.

Recently Koga *et al.*[13] considered the same two-band Hubbard model involving semi-circular densities of states with $W_1=2$ eV, $W_2=4$ eV and on-site Coulomb interactions specified by $U=U'+2J$. Also assuming both subbands to be half filled, they studied the effect due to larger Hund's rule coupling by choosing $J=U/4$ and $U'=U/2$. To be able to reach lower temperatures, the DMFT calculations were performed within the exact diagonalization (ED) method[14] and a linearized two-site version of the DMFT.[15] Surprisingly, both impurity treatments indicate the existence of orbital-selective metal insulator transitions, i.e., the narrow subband exhibits a smaller critical U_c than the wide subband, implying a region of coexisting metallic and insulating subbands in spite of the interorbital Coulomb interactions defined by U' and J.

The conflicting results obtained within these various approaches underline the subtle and complex nature of the Mott transition in multiorbital systems. Since the nonisotropic

multiband character among transition metal oxide materials is the rule rather than an exception there is evidently a need to clarify this fundamental issue. Further theoretical studies are required to test the reliability of the DMFT method and various quantum impurity treatments. Contradictory results for a rather simple model which nevertheless captures a key feature present in many real systems obviously shed doubts on predictions obtained for more complex materials.

In the present work we reconsider the same two-band Hubbard model as in Refs.11 and 13. Since the QMC calculations are difficult to perform at low temperatures, we consider first the simpler iterated perturbation theory at finite T. Although this scheme is not reliable on a quantitative level, it can serve as a useful guide for qualitative purposes. At sufficiently low temperatures, the IPT reveals a single first-order transition for both subbands, confirming our previous results. Because of the numerical simplicity of this model we are able to obtain the entire T-U phase diagram. We then study the same model within the two-band QMC method. Although convergence is considerably more difficult at low temperatures, these results also suggest a common Mott transition. On the other hand, the interpretation of this multiband phase transition is complicated since in both phases the subbands exhibit quite different correlation features due to their different single-particle properties. Thus, in the metallic phase, the narrow band is much more correlated than the wide band and shows a mixture of both metallic and insulating features. Similarly, in the insulating phase the narrow band exhibits a gap while the wide band reveals pronounced bad-metal behavior. Thus, the transition is partially incomplete for individual subbands. This complexity of the quasiparticle spectra, and the difficulty of clearly identifying metallic and insulating properties at finite temperatures, presumably is the origin of some of the contradictions between the previous works.

The outline of this paper is as follows. In the following section we discuss the DMFT results derived within the IPT as a function of temperature. Section III contains the results obtained for the QMC method. Section IV provides a summary.

II. IPT-DMFT

Let us consider the paramagnetic metal insulator transition in a two-band Hubbard model consisting of subbands of width $W_1=2$ eV and $W_2=4$ eV. The densities of states are assumed to be semicircular: $\rho_i(\omega)=4/(\pi W_i)(1-4\omega^2/W_i^2)^{1/2}$, corresponding to nonhybridizing Bethe lattices. Both bands are taken to be half filled. The interacting Green's functions at imaginary frequencies are defined as

$$G_i(i\omega_n)=\int d\omega \frac{\rho_i(\omega)}{i\omega_n+\mu-\omega-\Sigma_i(i\omega_n)}, \qquad (1)$$

where $\omega_{n\geqslant 0}=(2n+1)\pi k_B T$ are Matsubara frequencies and μ is the chemical potential. $\Sigma_i(i\omega_n)$ are the subband self-energies which must be determined self-consistently. Removal of the self-energy from the central site yields the impurity Green's functions

$$g_i(i\omega_n)=[G_i^{-1}(i\omega_n)+\Sigma_i(i\omega_n)]^{-1}. \qquad (2)$$

The corresponding Fourier transforms at imaginary times are denoted as $g_i(\tau)$. Since both bands are assumed to be symmetric and half filled, these functions satisfy the conditions $g_i(0)=g_i(\beta)=-0.5$ and $g_i(\tau)=g_i(\beta-\tau)$. For purely on-site Coulomb interactions specified by intraorbital and interorbital matrix elements, the self-energy components in second-order perturbation theory are:[6]

$$\Sigma_i(i\omega_n)=\int_0^\beta d\tau e^{i\omega_n\tau}[\sigma_1 g_i^3(\tau)+\sigma_2 g_i(\tau)g_j^2(\tau)], \qquad (3)$$

where $j=1(2)$ for $i=2(1)$ and the coefficients σ_i are defined as $\sigma_1=U^2$ and $\sigma_2=J^2+2(U'^2+J^2-U'J)$. Since we take both subbands to be half filled we do not consider here corrections to the bare second-order self-energy which should be introduced in the absence of particle-hole symmetry.[16] At half filling, the first-order Hartree-Fock terms are identical for both bands, $\Sigma_i^{\mathrm{HF}}=1.5\,U-2.5\,J$, and can be absorbed by the chemical potential. Throughout this paper we assume $J=U/4$ and $U'=U/2$, unless noted otherwise.

The self-energies $\Sigma_i(i\omega_n)$ are now inserted in Eq. (1) and the procedure is iterated until self-consistency is achieved. The starting self-energy is taken to be zero. In particular at low temperatures, the direct and inverse Fourier transforms must be done with sufficient accuracy.[17] Also, at each iteration the symmetry condition $g_i(\tau)=g_i(\beta-\tau)$ is enforced to remove spurious effects due to numerical inaccuracies. This ensures that the $\Sigma_i(i\omega_n)$ remain purely imaginary as they should be for symmetric half filled bands. Typically $L=256$ time slices and 2^{12} Matsubara frequencies were used. Also, the real-ω integration in Eq. (1) must be performed on a rather fine mesh in order to capture the narrow coherent peak close to the metal-insulator transition. This can be achieved by linearly interpolating $\rho_i(\omega)$ and performing the ω integral analytically between mesh points. Once a converged solution is found, the Green's functions $G_i(i\omega_n)$ are used to generate the Fourier transforms $G_i(\tau)$ from which the quasiparticle spectra at real frequencies are derived via the maximum entropy method.[10]

Figures 1–4 show the variation of the subband quasiparticle weights $Z_i\approx 1/[1-\mathrm{Im}\,\Sigma_i(i\omega_0)/\omega_0]$ as functions of U for various temperatures. Up to $T=0.04$ eV the results show the typical hysteresis behavior obtained also for the single-band Hubbard model.[7,17,18] If U is gradually increased from the metallic side the transition occurs at a slightly larger critical value than if one begins in the insulating phase and gradually decreases U. The hysteresis is most pronounced at low temperatures and becomes weaker as T increases. For $T\geqslant 0.05$ eV it is negligibly small and the transition begins to resemble the typical cross-over behavior.

The important point of these results is that the quasiparticle weights of the narrow and wide subbands exhibit first-order transitions at precisely the same critical $U_c(T)$. This picture supports our previous results suggesting a single Mott transition in a nonisotropic multiorbital environment, in contrast to the orbital selective transitions found in Refs.9 and 11. In line with the notation used in the single-band case,

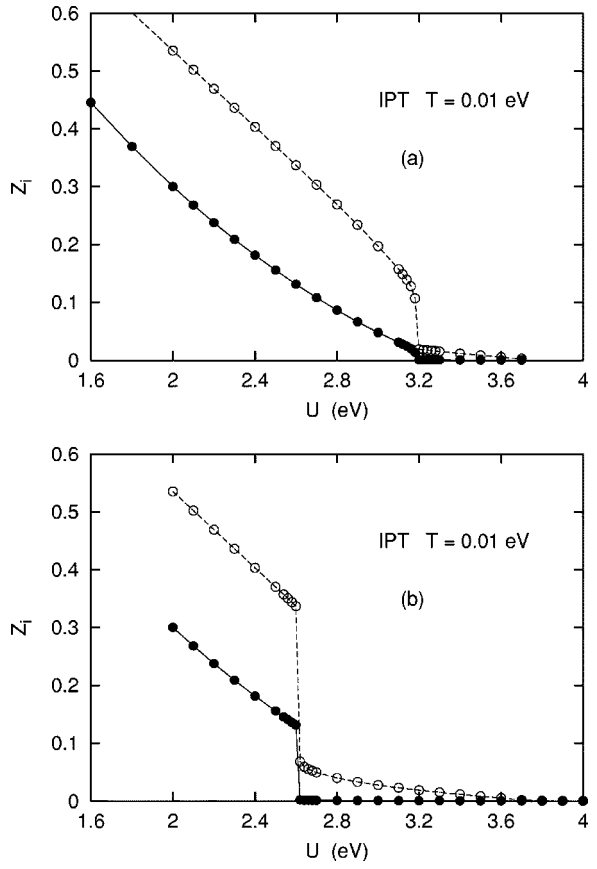

FIG. 1. Quasiparticle weights Z_i of two-band Hubbard model as a function of on-site Coulomb energy U for $T=0.01$ eV, calculated within IPT-DMFT. Solid (open) dots: Z_1 (Z_2). (a) Increasing U, (b) decreasing U.

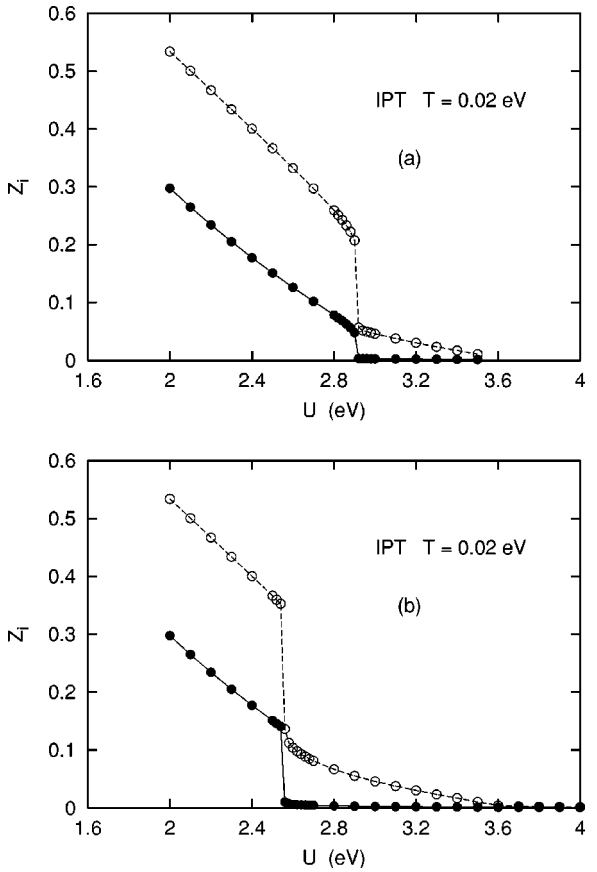

FIG. 2. Same as Fig. 1 except for $T=0.02$ eV.

we denote the common critical value for decreasing U as $U_{c1}(T)$ and for increasing U as $U_{c2}(T)$. (These values should not be confused with the critical U derived in Ref.11 for the isotropic two-band models.) For $T \leqslant 0.04$ eV the transitions are perfectly discontinuous both at $U_{c1}(T)$ and $U_{c2}(T)$. For $T \geqslant 0.05$ eV finite temperature broadening progressively dominates the transition region.

Figure 5 shows the phase diagram obtained from the functions $Z_i(T,U)$. The overall shape of the phase boundaries agrees well with those obtained for the single-band Hubbard model.[7,18] According to the single-band phase diagram, the actual first-order metal insulator transition takes place along an intermediate line $U_c(T)$ such that $U_{c1}(T) < U_c(T) < U_{c2}(T)$ (schematically indicated by the dashed curve). Extrapolation of the phase boundaries suggests a common transition temperature of about $T_c \approx 0.05$ eV. This value agrees well with the average between the critical temperatures derived for isotropic narrow and wide two-band systems, $T_{c11} \approx 0.033$ eV and $T_{c22} \approx 0.067$ eV, respectively. [In the single band case the IPT-DMFT yields $T_c/W \approx 0.02$.[7] According to Eq. (3), for doubly degenerate bands and $U=2U'=4J$, this value should be reduced by a factor $(\sigma_1+\sigma_2)^{1/2}/U \approx 1.2$.]

Although interorbital Coulomb interactions lead to a common metal-insulator transition in the narrow and wide subbands, it is clear from Figs. 1–4 that the subband quasiparticle weights differ greatly both in the metallic and insulating phases. In this sense, the subband transitions are partly incomplete: On the metallic side, Z_1 is consistently smaller than Z_2 because of the more pronounced correlations within the narrow band. As as result, as will be discussed below, this band can exhibit quasi-insulating behavior. Conversely, on the insulating side of the transition, Z_1 drops almost to zero while Z_2 drops to a finite intermediate value and gradually decreases towards larger U. This 'bad-metal' behavior of the wide band above the transition is weak at low temperatures but becomes more important towards T_c. There is no indication of a second first-order transition in the wide subband at larger U.

To analyze the subband quasiparticle properties close to the transition in more detail we show in Fig. 6 the self-energies $\Sigma_i(i\omega_n)$ for $T=0.02$ eV near $U_{c2}(T)$. Slightly below the transition at $U=2.91$ eV the wide band is clearly metallic with $\Sigma_2(i\omega_n) \sim \omega_n$ at small Matsubara frequencies. The narrow band exhibits significant deviations from this linear behavior. Only at the two lowest frequencies $\Sigma_1(i\omega_n)$ is roughly linear in ω_n. At larger frequencies it becomes inversely proportional to ω_n. Thus, this band is in the intermediate region between metallic and insulating behavior, exhibiting a narrow coherent peak near E_F nearly separated from pronounced Hubbard bands (see below). At $U=2.92$ eV, i.e., just above the transition, the narrow band has become fully insulating with $\Sigma_1(i\omega_n) \sim 1/\omega_n$. In contrast, $\Sigma_2(i\omega_n)$ approaches a constant in the limit of small ω_n. Thus, the wide

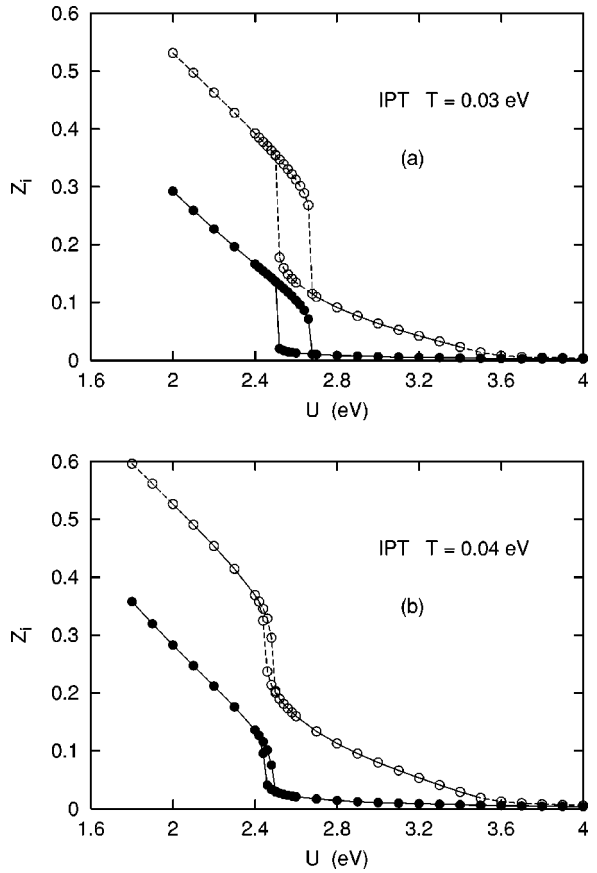

FIG. 3. Same as Fig. 1 except for (a) $T=0.03$ eV and (b) $T=0.04$ eV. Each figure shows the hysteresis obtained for increasing U (upper points) and decreasing U (lower points).

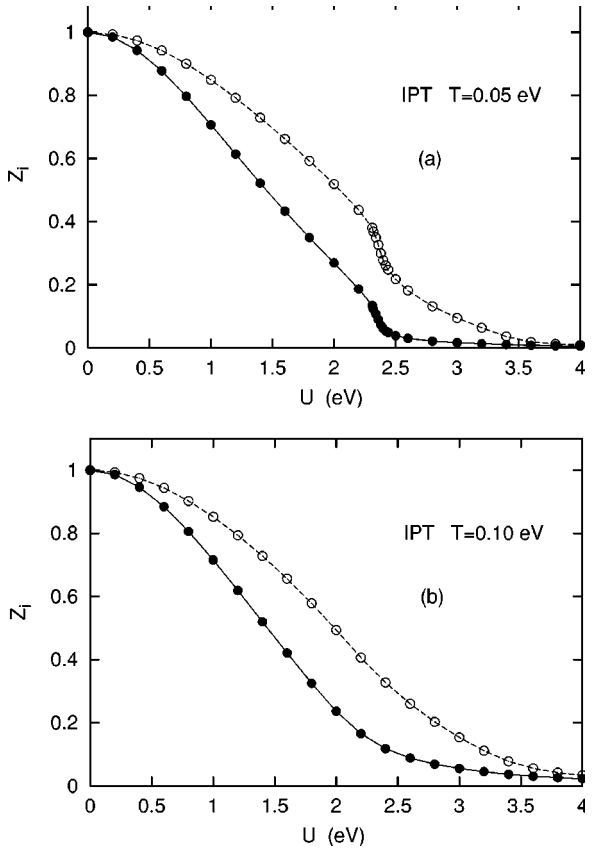

FIG. 4. Same as Fig. 1 except for (a) $T=0.05$ eV and (b) $T=0.1$ eV. Hysteresis effects are negligible at these temperatures.

band still is in the intermediate range between metallic and insulating behavior. These results demonstrate that in the vicinity of the Mott transition the two subbands exhibit a complicated superposition of different cross-over behaviors as they switch between the metallic and insulating phases.

The effect of these subband dependent correlations on the quasiparticle spectra is illustrated in Fig. 7 for $T=0.01$ eV just below and above $U_{c1}(T)$. On the metallic side, the wide band is perfectly metallic. The narrow band exhibits a very narrow coherent peak near E_F and nearly vanishing weight between this peak and the large Hubbard peaks.[19] Thus, the narrow band shows features indicative of both metallic and insulating behavior. Similarly, above the transition the coherent peak in $N_1(\omega)$ has vanished and a narrow excitation gap is visible. $N_2(\omega)$, on the other hand, still has appreciable spectral weight near the Fermi energy. According to the phase diagram, at sufficiently low temperatures the true first-order line $U_c(T)$ approaches the boundary $U_{c2}(T)$. In fact, within a consistent dynamical two-site approximation[20] $U_c(T)$ is only slightly smaller than $U_{c2}(T)$. Figure 1 shows that near this line the bad-metal character of the wide subband above the transition is much weaker than close to $U_{c1}(T)$.

The above results suggest that, although there is a single metal-insulator transition for both subbands, slightly below and above this transition the quasiparticle spectra are rather complicated, partially exhibiting "coexisting" metallic and insulating behavior. In fact, in the range $0.01\ \text{eV} \leqslant T \leqslant T_c$, the transition in the wide band might be more appropriately described as metal/bad-metal transition. However, this behavior is associated with the fact that at finite T there is no clear distinction between metal and insulator. Extrapolation

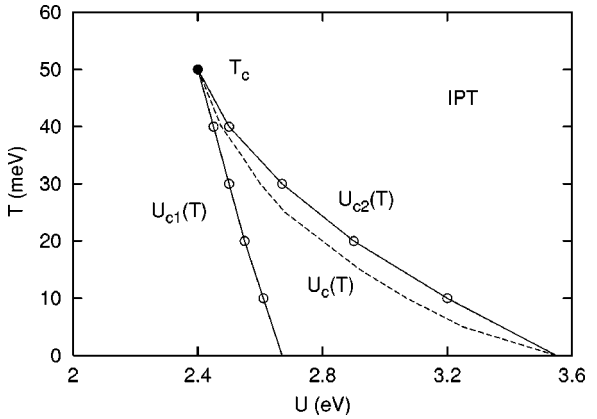

FIG. 5. Phase diagram for two-band Hubbard model, calculated within IPT-DMFT. Open dots: critical Coulomb energies $U_{c1}(T)$ and $U_{c2}(T)$ derived from Figs. 1–4. The lines are guides to the eye. Their extrapolation yields the common second-order critical point marked by a solid dot. The actual first-order line $U_c(T)$ at low temperatures lies between $U_{c1}(T)$ and $U_{c2}(T)$ and is sketched by the dashed line.

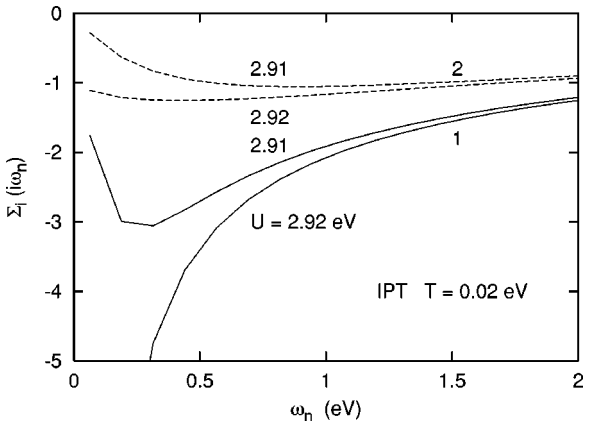

FIG. 6. Self-energy $\Sigma_i(i\omega_n)$ for two-band Hubbard model at $T=0.02$ eV near $U_{c2}(T)\approx 2.91$ eV at small Matsubara frequencies. Solid (dashed) curves: narrow (wide) subband.

of the results shown in Figs. 1–4 to even lower temperatures suggests that the bad-metal behavior in the wide band above $U_{c2}(T)$ eventually disappears and that the gaps in both bands open simultaneously at the same critical $U_c(T)$.

Before closing this section we briefly address the effect of the Hund's rule exchange coupling on the correlations within the two-band Hubbard model. The relatively large value assumed so far, $J=U/4$, gives rise to considerable anisotropy and is partly the origin of the qualitative differences between the subbands, in particular near the transition. The reason for these differences can be understood in terms of the self-energy expression given in Eq. (3). For $J=U/4$, $\sigma_2/\sigma_1 \approx 0.5$ while for $J=0$, $\sigma_2/\sigma_1=2$. Near the Fermi level the single-particle density of states scales with the band width, i.e., $g_1(\beta/2)=2g_2(\beta/2)$ before the Coulomb interaction is switched on. Thus for $J=U/4$, $\tau=\beta/2$ one finds: $\Sigma_1/\Sigma_2 = (\sigma_1 g_1^3+\sigma_2 g_1 g_2^2)/(\sigma_1 g_2^3+\sigma_2 g_2 g_1^2)=(8+0.5\times 2)/(1+0.5\times 4) = 3$ whereas for $J=0$: $\Sigma_1/\Sigma_2\approx(8+2\times 2)/(1+2\times 4)=4/3$. The subband contributions to the self-energy therefore differ significantly for $J=U/4$, but they are quite similar for $J=0$, giving rise to much more isotropic behavior.

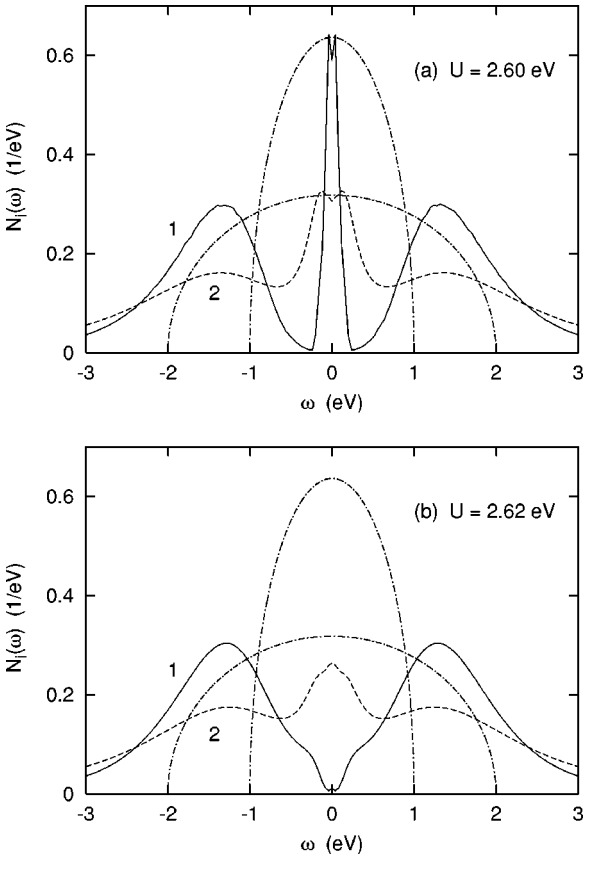

FIG. 7. Quasiparticle spectra $N_i(\omega)$ for two-band Hubbard model at $T=0.01$ eV near $U_{c1}(T)$. (a) Below the transition: $U=2.60$ eV; (b) above the transition:$U=2.62$ eV. Solid (dashed) curves: narrow (wide) subband: dash-dotted curves; bare densities of states.

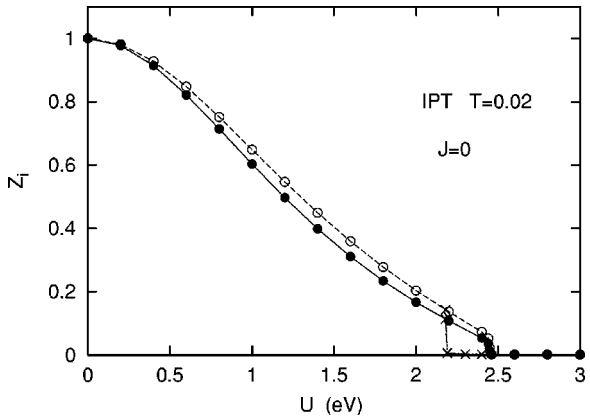

FIG. 8. Quasiparticle weights Z_i of two-band Hubbard model as a function of on-site Coulomb energy U for $T=0.02$ eV and $J=0$. Solid (open) dots: Z_1 (Z_2) for increasing U. Symbols (x) in the range 2.2–2.5 eV: $Z_1, Z_2\approx 0$ for decreasing U.

Figure 8 shows the quasiparticle weights Z_i as functions of U for $J=0$ at $T=0.02$ eV. The comparison with Fig. 2 demonstrates that as a result of the greater isotropy of the system the correlation induced reduction of quasiparticle weight is now quite similar for both subbands. In particular, slightly below and above the transition both bands show similar metallic and insulating behavior, respectively, in contrast to the much more complex superposition of quasimetallic and quasi-insulating behavior obtained for $J=U/4$. As before, both bands undergo a first-order metal-insulator transition at the same critical U. Since there is neither single-particle hybridization nor Hund's rule coupling between subbands, the common transition is entirely caused by the interorbital Coulomb interaction $U'=U$. Without this interaction, we would have $Z_1(U)\approx Z_2(2U)$ (slight differences arise as long as the temperature is held fixed). Thus, the critical Coulomb energies of the subbands would differ by the same factor as the band widths W_i. Figure 8 shows that U' enforces a single transition at an intermediate U_c. As in Fig. 2, Z_i exhibit similar hysteresis behavior: for decreasing U the critical Coulomb energy is $U_{c1}(T)\approx 2.19$ eV while for increasing U we find $U_{c2}(T)\approx 2.45$ eV.

III. QMC-DMFT

In our previous work[11] we considered the same two-band Hubbard model as above with $W_2=2W_1=4$ eV. DMFT cal-

culations based on the multiband QMC method were performed for a rather high temperature, $T=0.125$ eV, which corresponds to the cross-over region above the critical temperature T_c. For $J=0.2$ eV, the quasiparticle weights Z_i were found to differ significantly at intermediate Coulomb energies due to the different subband kinetic-energy terms. Nevertheless, with increasing U the Z_i merge again and, within some uncertainty associated with critical slowing down, become very small at about the same $U_c(T)$.

Figure 9 shows the quasiparticle weights Z_i as functions of U obtained from analogous QMC calculations for $J=U/4$, $U'=U/2$. In the cross-over region at high temperatures ($T=0.125$ eV) the larger anisotropy caused by the stronger Hund's rule coupling leads to a pronounced overall broadening of the transition region. This applies also to the isotropic two-band models with degenerate narrow or wide subbands. Nevertheless, in the anisotropic case (12) the Z_i approach one another with increasing U and exhibit qualitatively similar asymptotic behavior.

The results for $T=0.031$ eV shown in Fig. 9(b) exhibit much sharper transitions in the isotropic as well as nonisotropic two-band systems. (In the single-band case[7,18] $T_c^{\mathrm{QMC}}/T_c^{\mathrm{IPT}}\approx 0.75$. Assuming the same ratio for the two-band case we estimate from Fig. 5 for the nonisotropic model: $T_c^{\mathrm{QMC}}\approx 0.038$ eV.) In the nonisotropic case the overall behavior of the quasiparticle weights is remarkably similar to the IPT results discussed in the preceding section. While Z_1 drops almost to zero near $U_{c2}=2.1$ eV Z_2 drops to a finite value and then decreases gradually towards larger U. The characteristic kink in Z_2 becomes even more pronounced at $T=0.02$ eV (see + symbols). This change in slope of $Z_2(U)$ near U_{c2} suggests that both subbands undergo a common transition at the same Coulomb energy and that the wide subband exhibits pronounced bad-metal behavior above U_c.

The hysteresis behavior of the Z_i for $T=0.02$ eV is shown more detail in Fig. 9(c). While for increasing U both Z_i exhibit a change of slope near $U_{c2}\approx 2.1$ eV, for decreasing U the common transition occurs at $U_{c1}\approx 1.8$ eV. (The vertical line of dots at 1.8 eV indicates the iterations from the lower to the upper branch.) As in the case of the IPT, there is no evidence for a second transition in the wide subband at larger U.

As can be seen in Fig. 10, the self-energies $\Sigma_i(i\omega_n)$ close to the critical Coulomb energy derived within the QMC method are consistent with those obtained in the IPT (see Fig. 6). At $U\leqslant 2.4$ eV the wide band is in the cross-over region between metallic and insulating behavior. For $U=2.7$ eV $\Sigma_2(i\omega_n)$ becomes inversely proportional to ω_n, i.e., a gap opens up. The narrow band undergoes a similar cross-over behavior, except at slightly lower values of U.

Figure 11 shows the quasiparticle spectra for $T=0.031$ eV in the vicinity of the critical Coulomb energy. When the narrow band is about to open a gap, the wide band is still fairly metallic. Its own gap would be even smaller and is therefore readily filled by finite temperature tails extending from the Hubbard peaks towards the Fermi level. Only if U is increased to about 2.7 eV is the gap in the wide band large enough to not be obliterated by this temperature broadening.

The variation of $Z_i(U)$ with increasing U shown in Fig. 9(b) is qualitatively similar to the one obtained by Koga *et al.*[13] within the exact diagonalization treatment of the nonisotropic two-band model: Near $U_c\approx 2.6$ eV Z_1 practically vanishes while $Z_2(U)$ remains finite but shows a characteristic change in slope. At larger Coulomb energies Z_2 decreases gradually without any clear evidence for a subsequent metal-insulator transition. (U_c is somewhat larger than in our QMC

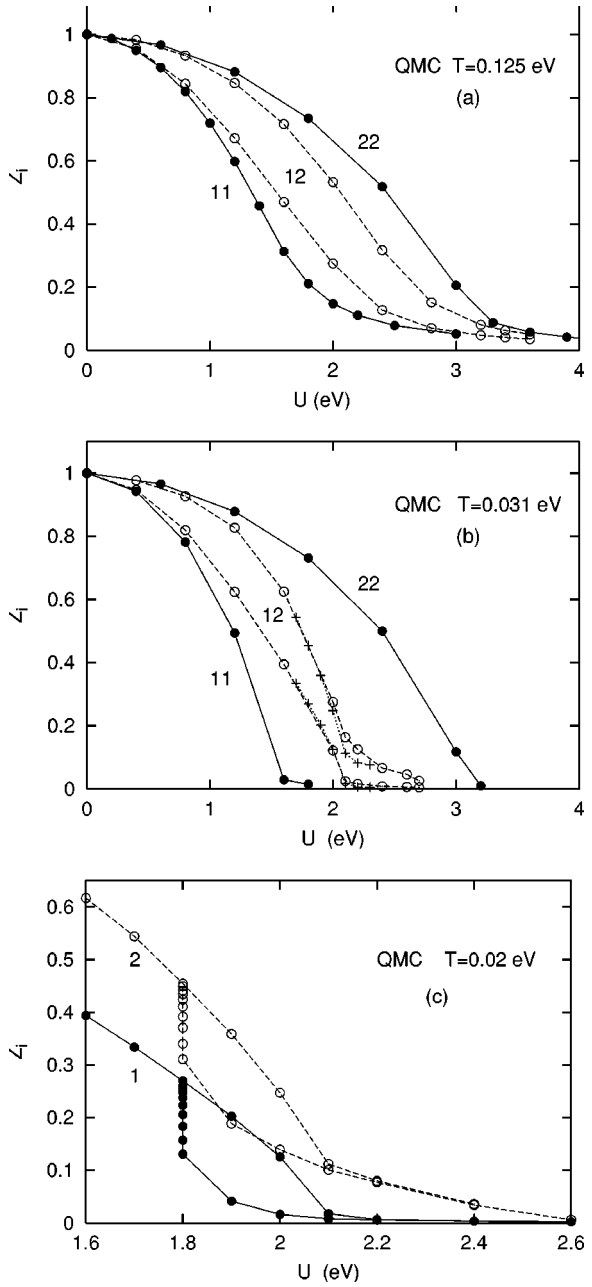

FIG. 9. Quasiparticle weights Z_i of two-band Hubbard models as functions of on-site Coulomb energy U calculated within the QMC-DMFT for $J=U/4$. (a) $T=0.125$ eV, (b) $T=0.031$ eV; solid dots: isotropic two-band models with degenerate narrow bands $W_i=2$ eV (11) or wide bands $W_i=4$ eV (22); open dots: nonisotropic two-band model with $W_2=2W_1=4$ eV (12). Symbols (+) in (b): results for $T=0.020$ eV. (c) Hysteresis obtained for nonisotropic model at $T=0.020$ eV; solid (open) dots: narrow (wide) band; upper (lower) points: increasing (decreasing) U. Lines are guides to the eye.

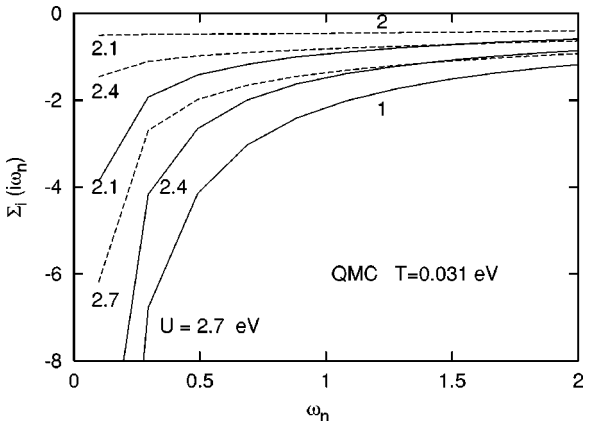

FIG. 10. Self-energy $\Sigma_i(i\omega_n)$ for two-band Hubbard model at $T=0.031$ eV near critical U at small Matsubara frequencies, calculated within QMC-DMFT. Solid (dashed) curves: narrow (wide) subband.

results since the ED calculations are carried out at near zero temperature. According to the phase diagram shown in Fig. 5 $U_{c2}(T)$ increases slightly with decreasing T.)

Since the ED-DMFT results are basically similar to our QMC-DMFT calculations, the different conclusions reached in Refs.11 and 13 seem to stem primarily from different interpretations of the underlying physics: In our view there is only one first-order transition, but with complex quasimetallic and quasi-insulating subband features just below and above this transition. This picture is based on the simultaneous discontinuous changes of the subband quasiparticle weights derived within the IPT-DMFT and the consistency between the IPT and QMC results. On the other hand, if the vanishing of the Z_i is used as a criterion, the subbands indeed behave very differently. Whereas for the narrow band a critical Coulomb energy can readily be identified, Z_2 falls off gradually and becomes negligibly small at much higher values of U. This metallic "tail" of Z_2 makes it difficult to identify a second critical Coulomb energy. According to our QMC and IPT results, this metallic tail should diminish at low temperature. It is not clear at present why the ED results in Ref. 13 show such a tail although they apply to near zero temperature. Also, it is not clear to what extent the different subband U_c's obtained within the two-site DMFT depend on the minimal one-level representation of the subband baths. The energy discretization inherent in both the ED and two-site methods plays a crucial role close to the transition when dynamical correlation effects on small energy scales are particularly important. It would be interesting to perform ED and two-site DMFT calculations in a wider range of temperatures in order to analyze the transition region in more detail.

IV. SUMMARY

The nature of the Mott transition in multiband systems was investigated within the dynamical mean-field theory. Although in practice subbands of transition metal oxides are usually coupled via single- as well as many-electron interactions, we focus here on the effect of interorbital matrix elements of the Coulomb energy, thus neglecting one-electron hybridization. In contrast to isotropic systems consisting of identical subbands, the metal-insulator transition in materials with coexisting narrow and wide subbands turns out to be remarkably complex. The present results confirm our previous finding, namely, the existence of a single transition rather than a sequence of orbital-selective transitions as the on-site Coulomb energy is increased. Nevertheless, at low but finite temperatures below the transition the narrow band reveals a narrow coherent peak nearly separated from the Hubbard bands. Conversely, above the transition the wide band shows pronounced bad-metal behavior. This coexistence of quasi-

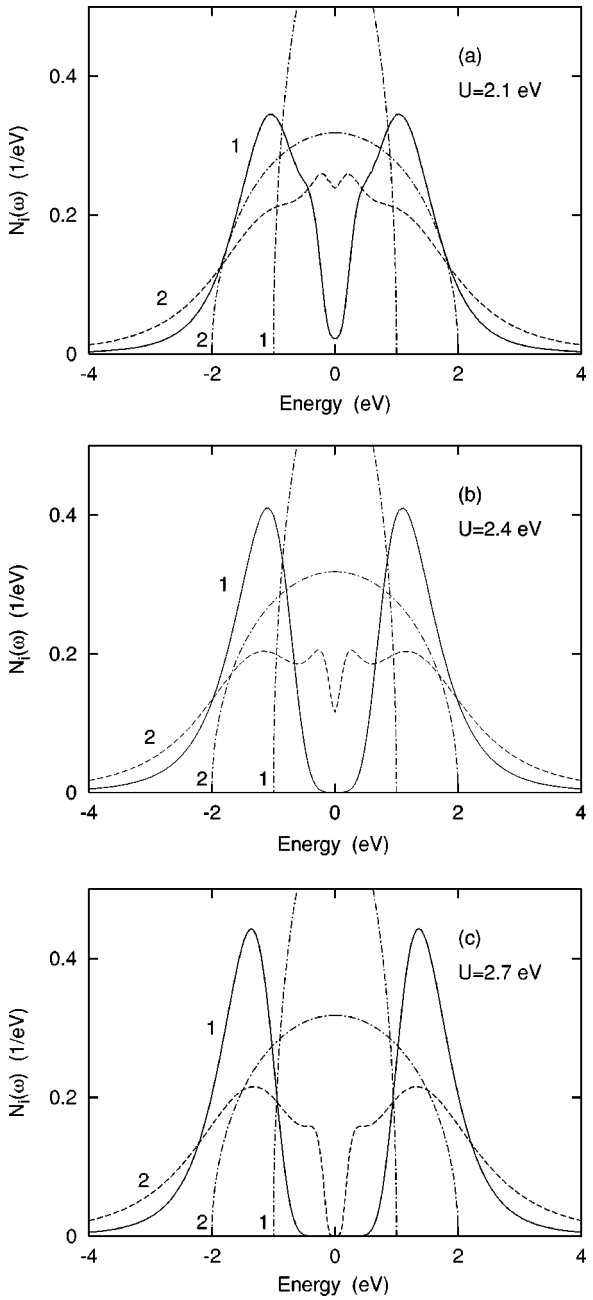

FIG. 11. Quasiparticle spectra $N_i(\omega)$ for two-band Hubbard model at $T=0.031$ eV, calculated within the QMC-DMFT. (a) $U=2.1$ eV; (b) $U=2.4$ eV; (c) $U=2.7$ eV. Solid (dashed) curves: narrow (wide) subband; dash-dotted curves: bare densities of states.

metallic and quasi-insulating spectral features in the vicinity of the transition makes the interpretation of the DMFT results nontrivial and partly explains the contradictory findings in Refs. 11 and 13.

Since it is difficult to perform QMC calculations at very low temperatures, we have carried out extensive DMFT calculations within the IPT. The phase diagram is consistent with earlier results obtained for single-band models. In particular, the quasiparticle weights show the typical hysteresis behavior giving rise to two first-order lines $U_{c1}(T)$ and $U_{c2}(T)$ defining the stability boundaries of the insulating and metallic regions, respectively. For $T \leqslant 0.01$ eV the results suggest that above the transition the metallic states in the wide band should disappear, i.e., that the excitation gaps in both bands should open at the same $U_c(T)$. At intermediate temperatures below T_c the IPT results are consistent with the QMC calculations: The quasiparticle weights in both subbands undergo simultaneous first-order transitions at $U_{c1}(T)$ or $U_{c2}(T)$. These transitions, however, are not complete in one or the other of the subbands. For instance, the wide band shows appreciable metallicity above the transition. Similarly, the narrow band exhibits partly insulating Hubbard peaks below the transition. This mixture of metallic and insulating behavior diminishes towards low temperatures, i.e., purely metallic or insulating phases should evolve in both subbands.

Note added in proof. As recently pointed out in Ref. 21, a possible source of discrepancy between the QMC and ED results might be the different treatment of Hund's rule coupling terms. While ED includes both isotropic and nonisotropic elements, the latter are ignored in QMC to avoid sign problems at low temperatures. We note, however, that the full J matrix in Ref. 21 yields a variation $Z_i(U)$ that is remarkabley similar to the one shown in Fig. 9. Also, the IPT calculations in the present work are based on the full J matrix.

ACKNOWLEDGMENTS

I would like to thank A. Bringer for useful discussions. I also thank V. Oudovenko for sharing his subroutines for imaginary time/frequency Fourier transforms.

*Electronic address: a.liebsch@fz-juelich.de

[1] T. Oguchi, Phys. Rev. B **51**, 1385 (1995); I. I. Mazin and D. Singh, Phys. Rev. Lett. **79**, 733 (1997).
[2] Y. Maeno, T. M. Rice, and M. Sigrist, Phys. Today **54**, (1)42 (2001).
[3] S. Nakatsuji and Y. Maeno, Phys. Rev. Lett. **84**, 2666 (2000).
[4] P. Zhang W.Luo, V. Crespi, M. Cohen, and S. Louie, Phys. Rev. B **70**, 085108 (2004).
[5] A. Liebsch, Europhys. Lett. **63**, 97 (2003).
[6] A. Liebsch and A. I. Lichtenstein, Phys. Rev. Lett. **84**, 1591 (2000).
[7] For a review, see: A. Georges, G. Kotliar, W. Krauth, and M. J. Rozenberg, Rev. Mod. Phys. **68**, 13 (1996).
[8] A. Fang and K. Terakura, Phys. Rev. B **64**, R020509 (2001).
[9] V. I. Anisimov, I. A. Nekrasov, D. E. Kondakov, T. M. Rice, and M. Sigrist, Eur. Phys. J. B **25**, 191 (2002).
[10] M. Jarrell and J. E. Gubernatis, Phys. Rep. **269**, 133 (1996).
[11] A. Liebsch, Phys. Rev. Lett. **91**, 226401 (2003).
[12] A. Georges and G. Kotliar, Phys. Rev. B **45**, 6479 (1992).
[13] A. Koga, N. Kawakami, T. M. Rice, and M. Sigrist, Phys. Rev. Lett. **92**, 216402 (2004).
[14] M. Caffarel and W. Krauth, Phys. Rev. Lett. **72**, 1545 (1994).
[15] M. Potthoff, Phys. Rev. B **64**, 165114 (2001).
[16] H. Kajueter and G. Kotliar, Phys. Rev. Lett. **77**, 131 (1996).
[17] J. Joo and V. Oudovenko,Phys. Rev. B **64**, 193102 (2001).
[18] R. Bulla, T. A. Costi, and D. Vollhardt, Phys. Rev. B **64**, 045103 (2001); N. Bluemer, Ph. D thesis, 2003.
[19] The tiny dips near E_F are presumably not physical and stem from uncertainties of the maximum entropy method.
[20] M. Potthoff, Eur. Phys. J. B **36**, 335 (2003).
[21] A. Koga, N. Kawakami, T. M. Rice, andM. Sigrist, cond-mat/0406457 (unpublished).